RSC Advances

ROYAL SOCIETY OF CHEMISTRY

www.rsc.org/advances

Journal Name

RSCPublishing

ARTICLE

Polymeric Organo-Magnesium Complex for Room Temperature Hydrogen Physisorption

Cite this: DOI: 10.1039/x0xx00000x

Kapil Pareek,[a] Rupesh Rohan,[a] and Hansong Cheng [a,b] ,

Received 00th January 2012,
Accepted 00th January 2012

DOI: 10.1039/x0xx00000x

www.rsc.org/

We report a facile synthesis of a polymeric organo-magnesium complex (MTF-Mg) by reacting Mg-modified-melamine with terephthaldehyde for room temperature hydrogen physisorption. The pre-modification of melamine allows incorporation of exposed magnesium sites into the complex. The synthesized MTF-Mg complex exhibits a moderate BET surface area up to 137 $m^2 g^{-1}$ and a Langmuir surface area up to 222 $m^2 g^{-1}$. In this complex, magnesium metal sites act as the active sites for molecular hydrogen adsorption via an electrostatic interaction. The material shows a high isosteric heat of adsorption up to 12 kJ mol^{-1} and a maximum excess hydrogen uptake up to 0.8 wt % at 298K and 100 atm, comparable to the values of high surface area MOFs with exposed metals sites under similar conditions. The role of the exposed metal sites in enhancing hydrogen uptake capacity and isosteric heat of adsorption is demonstrated experimentally.

Introduction

Materials containing exposed metal sites have been a subject of great interest in recent years due to their potential applications in the field of gas adsorption,[1-14] catalysis[15-18] and sensor technologies.[19-21] The exposed metal sites are particularly well suited for adsorption of molecular hydrogen for applications at near ambient temperature.[2, 22] Recently, several metal organic framework (MOF) compounds with exposed metals have been discovered for potential hydrogen storage via physisorption.[1-10, 23] These materials exhibit considerably stronger interactions with molecular hydrogen than the van der Waals forces due to polarization of hydrogen molecules upon adsorption on the metal sites, as supported by both computational and experimental studies.[24-27] As a consequence, these compounds exhibit higher heat of hydrogen adsorption than the materials without exposed metal sites.[2, 4, 26] A thorough thermodynamic analysis indicates that a hydrogen binding enthalpy in the range of 15-20 kJ mol^{-1} would give the best balance between the storage capacity and the energy required to release the hydrogen at near ambient temperatures.[28]

In general, the exposed metal sites can be generated in a material by removal of metal bonded solvent molecules under an elevated temperature and high vacuum conditions.[2, 3] Alternatively, pre- or post-modification routes with metallic precursors can lead to generation of exposed metal sites into the framework materials.[2, 29, 30] The later method is deemed to facilitate incorporation of exposed metal sites into porous organic framework (POF) materials[31-34] and to give rise to an enhanced sorbate-sorbent interaction with a better hydrogen storage capacity at room temperature.

Recently, a POF material synthesized via a reaction of melamine with terephthaldehyde was reported with a high BET surface area ranging from 300 to 1337 $m^2 g^{-1}$ and high porosity.[35, 36] The reported melamine-terephthaldehyde framework (MTF) complex exhibits high structural and thermal stabilities due to its highly cross-linked nature. Unfortunately, the MTF compound exhibits a negligible hydrogen uptake at room temperature due to lack of active metal sites and the weak sorbate-sorbent interaction.

In this paper, we report a facile synthesis of a Mg functionalized melamine-terephthaldehyde framework (MTF-Mg) material via pre-modification for room temperature hydrogen physisorption. The synthesis of MTF-Mg was done by reacting Mg-modified-melamine with terephthaldehyde, following the reported procedure.[35, 36] The pre-modification of melamine was achieved using a dibutyl magnesium reagent.[37] The selection of Mg metal for the functionalization was motivated by the observed excess hydrogen storage capacity of 0.42 wt% at 298K and an isosteric heat of adsorption of 10.3 kJ mol^{-1} of MOF-74 with exposed Mg sites.[38] In the MTF-Mg complex, the highly rigid and structurally stable cross-linked

framework should offer a stable chelated ligand environment and a high exposure of Mg cations to hydrogen gas, which might lead to an enhanced hydrogen storage capacity at 298K and a strong sorbate-sorbent interaction. The experimental demonstration may shed a light on design of new adsorbent materials for high capacity hydrogen storage via physisorption at near ambient temperature conditions.

Experimental

Materials

Melamine (Sigma Aldrich), 1,4-benzenedicarboxaldehyde (Alfa Aesar), di-butyl magnesium (Sigma Aldrich), tetrahyrofuran (THF) (RCI labscan), dichloromethane (Sigma Aldrich), acetone (Sigma Aldrich), and diglyme (Sigma Aldrich). All chemicals were of an analytical grade and thus used without further purification. THF, acetone and dichloromethane were dried before use.

Synthesis of MTF-Mg complex

The MTF-Mg polymeric organo-magnesium complex was synthesized in a two-step reaction, as shown schematically in Scheme 1. In the first step, a flame-dried three neck flask fitted with a condenser and a magnetic stirring bar was charged with melamine (500 mg, 3.96 mmol) and a hexane (40 ml) solvent under argon atmosphere at -78 ^{o}C. Subsequently, di-butyl magnesium (5.94 mmol) was injected into the flask and stirred for 12 hrs under argon atmosphere, producing the Mg-modified-melamine complex and butane gas. In the second step, 1,4-benzenedicarboxaldehyde (796 mg, 5.94 mmol) and diglyme (40 ml) were added into the reaction mixture, which was then stirred at 160 ^{o}C for 72 hrs under argon atmosphere. Upon cooling to room temperature, the precipitated MTF-Mg was filtered and washed with an excess of anhydrous acetone, anhydrous tetrahydrofuran, and anhydrous dichloromethane, respectively. The solvents were removed under a reduced pressure by using a rotary evaporator. Final drying was done at 190 ^{o}C under vacuum in a tube furnace to produce a yellow powder with a yield of 70 %. FTIR (MTF-Mg): ῡ (triazine ring) 1550 cm^{-1}, 1480 cm^{-1}, ῡ (adsorbed moisture) 3200-3400 cm^{-1} (b).

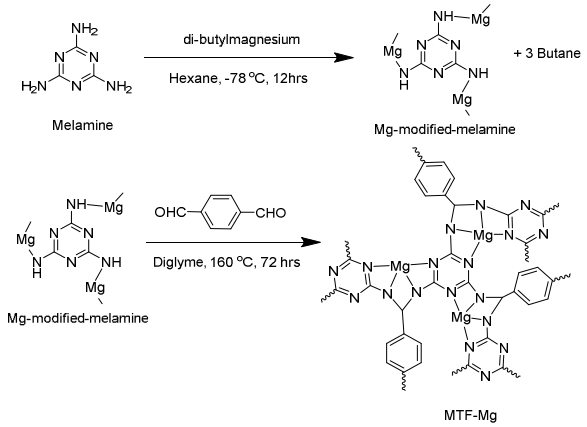

Scheme 1: The synthetic protocol of the MTF-Mg complex.

Characterization

Elemental analysis and ICP measurement were performed on Vario Micro Cube CHNX analyzer and Optima 5300 DV ICP-OES, respectively. Powder X-ray diffraction (XRD) was performed on a D5005 Bruker AXS diffractometer with Cu-Kα radiation (λ = 1.5410 A^{o}) at room temperature. The diffraction pattern of the MTF-Mg complex was measured using a sample size of 70-110 mg. SEM images were obtained using a scanning electron microscopy (SEM) with Jeol JSM-6701F. Samples were prepared by gold sputtering under 9Pa at room temperature (20s, 30mA) with a JEOL JFC 1600 Fine Coater. All X-ray photoelectron spectra (XPS) were taken with a VG Scientific ESCALAB MKII spectrometer. Infrared spectroscopy was taken on the Varian resolutions (version 4.0.5.009). Thermogravimetric analysis was performed on a TA instrument 2960 (DTA-TGA) from room temperature to 1000 ^{o}C at the heating rate of 5 ^{o}C/ min.

Hydrogen gas adsorption measurement

Gas adsorption isotherms were obtained on a computer-controlled commercial Gas Reaction Controller (GRC) manufactured by Advanced Materials Corporation. The GRC instrument is based on a volumetric method to determine gas adsorption and was calibrated by following the standard practice guidelines recommended by US DOE.[39] The empty sample chamber was tested to determine its zero adsorption baselines at 298K and 77K, respectively (ESI Fig. S1). Furthermore, the GRC was also calibrated with commercially available standard materials such as basolite A100 (MIL53-Al MOF) and $LaNi_5$ alloy at 77K and 298K, respectively (ESI Figs. S2 and S3). High purity H_2 (99.9995) gas was used for the adsorption measurements.

All gas adsorption-desorption measurements were performed following the standard procedure.[7, 9, 40] Around 300 mg of MTF-Mg was sealed in a sample chamber inside a glove box to prevent an exposure to moisture and was subsequently activated at 150 ^{0}C under a reduced pressure (below 10^{-5} torr) for overnight on the GRC. The adsorption-desorption isotherms of the MTF-Mg complex were measured at 323K and 298K over the pressure range of 0-100 atm.

The skeleton density of the compound was measured using a Quantachrome Ultrapyc 1200e instrument, which was calibrated using a sphere with a known volume (0.0898 cc). The skeleton density of the MTF-Mg complex (1.6 g cm^{-3}) was provided to the GRC to obtain an accurate void space volume by subtracting the skeleton volume of the sample from the volume of the sample chamber.

Enthalpy of adsorption

Enthalpies of adsorption were derived from the Clausius-Clapeyron equation.[26]

$$\left[\frac{\partial \ln p}{\partial\left(\frac{1}{T}\right)}\right]_{\theta} = \frac{\Delta_{ad}H}{R} \quad (1)$$

where T represents the temperature, p is the pressure (in kPa), $\Delta_{ad}H$ is the enthalpy of adsorption and R is the universal gas constant. [26] A plot of ln*p* against 1/T is a straight line of the slope $\Delta_{ad}H/R$ at a given surface coverage.

Nitrogen gas adsorption

Nitrogen gas adsorption-desorption isotherms were performed using a Micromeritics ASAP 2020 instrument. In a typical measurement, around 300 mg sample was transferred to a pre-weighted tube under inert atmosphere to prevent an exposure of the sample from moisture. The sample was activated under dynamic vacuum at 120 °C. The warm and cold free space corrections were performed for the sample using ultra-high-purity He gas (purity 99.9995%). N_2 adsorption-desorption isotherms were measured in a liquid nitrogen Dewar bath at the maximum pressure range of 1 atm.

The average number of adsorbed H_2 per Mg centre

The average number of adsorbed hydrogen molecules per Mg centre in the MTF-Mg complex was estimated based on the Mg% obtained from elemental analysis data provided in Table 1. The MTF-Mg complex adsorb 0.7 wt% of hydrogen at 298K and 100 atm, which corresponds to 0.7 g (0.347 mol) hydrogen for 100 g sample. The MTF-Mg complex has 12.84 % of Mg (0.528 mol) in the sample. Therefore, on average each Mg metal centre holds 0.65 molecules of H_2.

Results and discussions

Table 1. Elemental analysis results of the MTF-Mg complex.

Compound		C%	H%	N%	Mg%
MTF-Mg	Expected	45.94	2.97	35.74	15.50
	Found	35.94	3.89	28.54	12.84

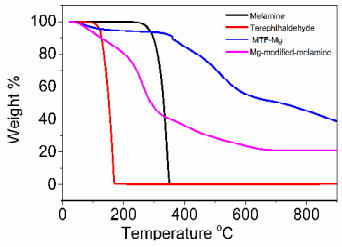

Figure 1. The TGA thermograms of melamine (black), terephthaldehyde (red), MTF-Mg (blue) and Mg-modified-melamine (pink) under nitrogen atmosphere at the 5 °C/min heating rate.

The elemental analysis data for the MTF-Mg complex is tabulated in Table 1. Due to the cross-linked polymeric nature of the MTF-Mg complex, it is difficult to assign an accurate empirical formula unit to the material, which results in the discrepancy in the elemental analysis data.[35, 36] The TGA thermograms of the starting materials and the MTF-Mg compound are displayed in Fig. 1. The MTF-Mg complex shows a steep weight loss at ca. 468 °C, higher than the degradation temperatures of melamine (330 °C), Mg-modified-melamine (264 °C) and terephthaldehyde (163 °C) under nitrogen atmosphere. The higher thermal stability supports the expected polymerization reaction between the Mg-modified-melamine precursor and terephthaldehyde. In addition, the MTF-Mg complex displays a steady weight loss and a char residue of 19% at 1000 °C.

FTIR measurement of terephthaldehyde, melamine and MTF-Mg was done and results are depicted in the Fig. 2. In the spectra of MTF-Mg, the characteristic bands of –CHO functional groups at 2870 (C-H str.) and 1690 cm^{-1} (C=O str.) and the sharp bands of melamine at 3419, 3470 cm^{-1} (NH_2 str.) and 1650 cm^{-1} (NH_2 defor.) are absent or having low intensity, indicating a success of the condensation reaction.[35, 41] In addition, the appearance of a broad band at 3200-3400 cm^{-1} is attributed to the adsorbed moisture during sample preparation. The absorption bands at 1550 and 1480 cm^{-1} are attributed to the C=N stretch of the triazine ring of the MTF-Mg complex.

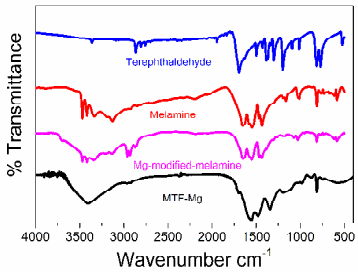

Figure 2. The FTIR spectra of terephthaldehyde (blue), melamine (red), Mg-modified-melamine (pink) and MTF-Mg complex (blue).

The X-ray photoelectron spectra (XPS) of the MTF-Mg complex are shown in Fig. 3. The carbon 1s binding energy of 284.8 eV has been used to calibrate the binding-energy scale for the XPS measurements as recommended by National Institute of Standards and Technology (NIST) database.[42] The C1s peak (Fig. 2a) can be fitted into four peaks, corresponding to the carbon atoms in the benzene ring (283.63 eV), the linkers (the carbon atom bonded to the more electronegative N or O atoms 284.98, 287.10 eV) and the triazine ring (288.60 eV), respectively.[43, 44] The peak for the O1s band is due to the C-OH group formed during the condensation reaction and some un-reacted C=O groups of the terephthaldehyde monomer.[35] The N1s band can be fitted into three peaks at 396.31, 397.56 and 398.81 eV. The peak at 396.31 eV corresponds to the nitrogen atoms of the triazine ring (C=N-C) and the remaining two peaks at 397.56 and 398.81 eV are associated with the nitrogen atoms of the amine groups coordinated to the magnesium metals.[35] The energy band of Mg 2p can be approximately fitted into a group of the three peaks located at 50.33, (Mg bonded with the O containing groups) 51.26 (Mg–N) and 52.38 eV, (Mg–N),

respectively (Fig. 3c), reflecting different chemical environments. The high binding energy of the Mg 2p peaks is attributed to the high electronegativity of the nitrogen atoms and the delocalization of the charges, derived from the ionic N–Mg bonds, into the aromatic ring.

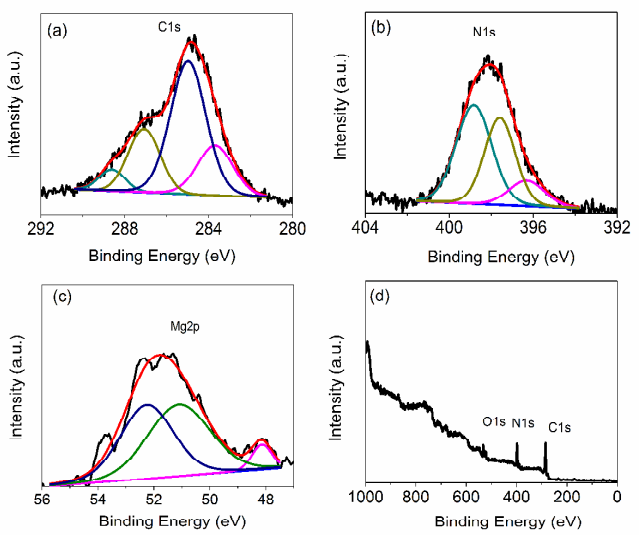

Figure 3. The X-ray photoelectron spectra of the MTF-Mg copolymer (a) high resolution scan of C1s, (b) high resolution scan of N1s, (c) high resolution scan of Mg2p, and (d) a complete scan.

Nitrogen gas adsorption-desorption isotherms of the complex was collected at 77 K and 1 atm pressure (Fig. 4). Notably, the MTF-Mg complex exhibits a Type IV adsorption isotherm with a small desorption hysteresis, confirming the mesoporous nature of the material. The compound displays a BET surface area of 137 $m^2 g^{-1}$ and a Langmuir surface area of 222 $m^2 g^{-1}$, respectively. The surface area of MTF-Mg is lower than the reported values of the melamine-terephthaldehyde based network compounds without metal incorporation (300-1377 $m^2 g^{-1}$ g), [35, 45, 46] most of MOF materials (150-5000 $m^2 g^{-1}$)[26] and porous carbons (100-1500 $m^2 g^{-1}$).[47] The relatively low surface area of the MTF-Mg complex is attributed to the functionalization of the organo-magnesium moiety. The DFT pore size distribution of the MTF-Mg complex (Fig. 4b) clearly indicates the presence of a wide range of nano-pores with the main pore size of about 18 Å.

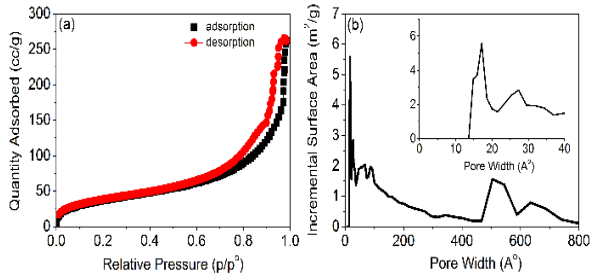

Figure 4. (a) The nitrogen adsorption-desorption isotherms at 77K for MTF-Mg, (b) the pore size distribution calculated from the nitrogen isotherm at 77K by applying a DFT pore size analysis method.

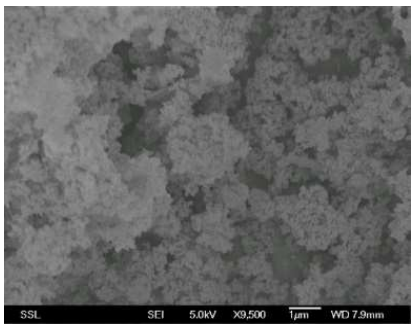

Figure 5. The SEM micrograph of MTF-Mg copolymer.

The porous structure of the MTF-Mg complex was further investigated by scanning electron microscopy (SEM). The SEM micrograph confirms that the MTF-Mg has loosely packed agglomerates and the wide pore size distribution is attributed to the inefficient packing of these agglomerates with a lack of topological self-complementarity (Fig 5).[48] These amorphous, loosely packed structures are important for enhancing the accessibility of gas molecules to the active sites of the material.[35]

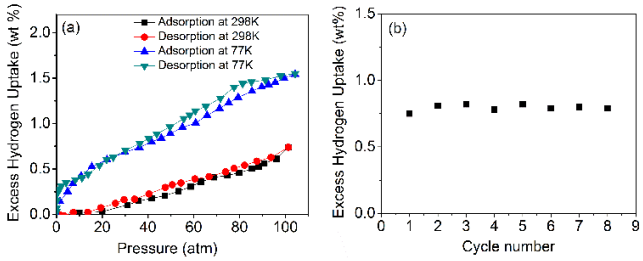

Figure 6. (a) The excess hydrogen uptake of MTF-Mg, and (b) the excess hydrogen uptake at 298K and 100 atm in eight fully reversible adsorption-desorption cycles in MTF-Mg.

The hydrogen adsorption-desorption isotherms of the MTF-Mg complex are shown in Fig. 6a. The isotherm at 77K increases linearly without saturation. The linear adsorption isotherm at 77K with the applied pressure has already been commonly seen in the low surface area Kubas type metal hydrazide gel materials.[5-8] On the other hand, in most of the high surface area physisorption-based materials, the adsorption curve shows a saturation capacity reflected as the "Knee point" in the isotherm. We note here that the adsorption mechanism of the low surface area Kubas type gel materials and thus the MTF-Mg complex is characteristically different from that of the high surface area adsorbents where the Chahine's rule,[49] which states that hydrogen uptake at 77K is about 1 wt% per 500 $m^2 g^{-1}$ applies and the adsorption is governed by the van der Waals interaction between H_2 and the host surfaces.[49] Here, with the low surface area of MTF-Mg, the linear adsorption curve at 77K is attributed to adsorption of H_2 molecules mainly on the exposed metal sites with a much stronger interaction. To rule out a linear increase of uptake upon gas compression, the apparatus with an empty sample chamber was thoroughly calibrated at 100 atm prior to the test (Fig. S1). At 298K and 100 atm, the MTF-Mg

complex exhibits a maximum hydrogen storage capacity of 0.8 wt%, comparable to the previously reported values of MOFs with exposed metals[2, 4, 26] and some of the metal hydrazide gel materials.[5-8] It should be noted that despite 5 folds lower metal loading in MTF-Mg than in the Kubas type gel materials (12.84 vs 50-80), the excess hydrogen uptake capacity is still comparable to the values observed in many Kubas type compounds mainly due to the relatively higher exposure of Mg cations in the MTF-Mg. The reversibility of hydrogen storage in the MTF-Mg complex and the cyclic stability were confirmed by eight fully reversible hydrogen adsorption-desorption cycles at 298K and 100 atm (Fig. 6b).

To quantitatively describe the adsorption strength, the isostearic heat of adsorption (Qst) was derived from the measured isotherms at 298K and 323K (Fig.7). The results confirm the low coverage Qst up to 13.2 kJ mol^{-1} calculated from the Clausius-Clapeyron equation and 12 kJ mol^{-1} calculated from the Virial method, higher than the reported heats of adsorption for H_2 in MOFs with exposed metal sites. The high Qst supports the strong host-H_2 interaction and the high hydrogen storage capacity of the complex at 298K.

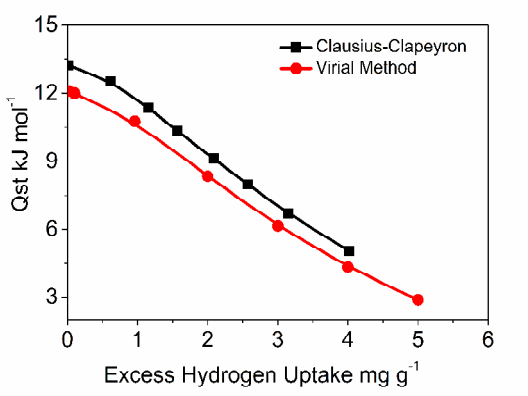

Figure 7. Calculated isostearic heat of adsorption of H_2 on MTF-Mg from the isotherms at 298K and 323K, using the Clausius-Clapeyron equation and Virial method.

Figure 8 depicts the comparison between MTF-Mg and a set of H_2 physisorption MOF materials with exposed metal sites. Clearly, MTF-Mg displays higher Qst value than the exposed metal site MOFs, attributed to the relatively high exposure of the Mg metal sites in MTF-Mg. We note that among these materials, the surface area of MTF-Mg is the lowest but yet the compound exhibits comparable gravimetric hydrogen density. In comparison to the exposed Mg sites in MOF-74, the extra framework Mg cations in the MTF-Mg complex are relatively more exposed and thus enable a higher excess hydrogen uptake at 298K and a higher Qst value. Unfortunately, the relatively low surface areas and the lack of complete exposure of the cations may prevent these materials from storing molecular hydrogen with a higher capacity at room temperature. Nevertheless, this experimental demonstration represents a new direction for search of better materials for hydrogen storage via physisorption.

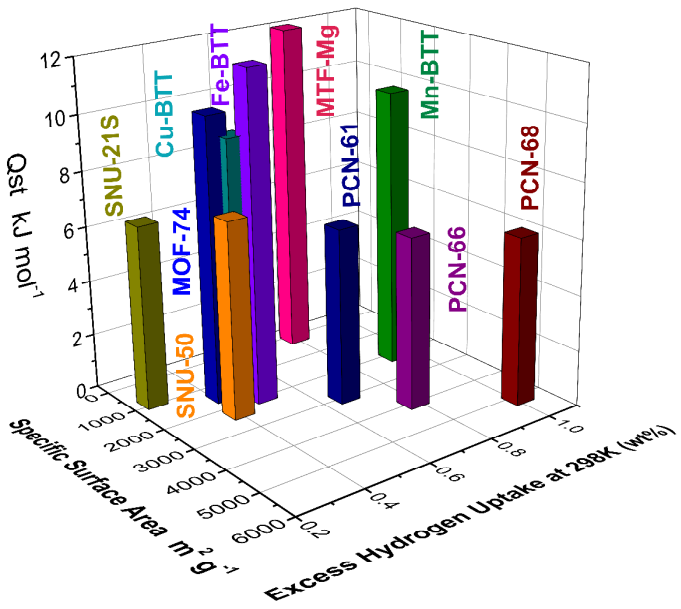

Figure 8. A comparison of excess hydrogen storage capacity, surface area and isosteric heat of adsorption of several exposed metal site MOFs and MTF-Mg materials of present work.

Conclusions

We have presented a facile synthesis protocol of a polymeric organo-magnesium complex with exposed magnesium metal sites for room temperature hydrogen storage via physisorption. The synthesized MTF-Mg complex exhibits a relatively moderate BET specific surface area of 137 $m^2 g^{-1}$, lower than most of contemporary hydrogen physisorption materials. Remarkably, owing to the high exposure of the magnesium metal sites, the compound exhibits a higher isosteric heat of adsorption of 12 kJ mol^{-1} than the MOF materials with exposed metal sites with a comparable hydrogen uptake capacity of 0.8 wt% at 298K and 100 atm pressure. The hydrogen storage capacity of MTF-Mg is lower than what has been reported in some of the Kubas type gel materials mainly due to its lower number of exposed metal sites. High hydrogen capacity at 298K is thus envisaged if the surface area can be significantly enhanced and more exposed metal sites can be placed in the polymeric compound. Nevertheless, the experimental demonstration of the interaction between an exposed cation and H_2 is important for future development of more effective materials to store hydrogen at near ambient temperature via physisorption.

Acknowledgements

The authors gratefully acknowledge support of a Start-up grant from NUS, a POC grant from National Research Foundation of Singapore, a Tier 1 grant from Singapore Ministry of Education and the National Natural Science Foundation of China (No.

21233006). We thank Prof. Dan Zhao for stimulating discussions and for his assistance of pore size measurement.

Notes and references

a Department of Chemistry, National University of Singapore, Singapore.117543; E-mail: chghs2@gmail.com
b Sustainable Energy Laboratory, China University of Geoscience, Whuan 430074, China.

Electronic Supplementary Information (ESI) available: [Instrument calibration, PXRD].

1. X. Lin, I. Telepeni, A. J. Blake, A. Dailly, C. M. Brown, J. M. Simmons, M. Zoppi, G. S. Walker, K. M. Thomas, T. J. Mays, P. Hubberstey, N. R. Champness and M. Schröder, *J. Am. Chem. Soc.*, 2009, **131**, 2159-2171.
2. M. Dincă and J. R. Long, *Angew. Chem. Int. Ed.*, 2008, **47**, 6766-6779.
3. J. G. Vitillo, L. Regli, S. Chavan, G. Ricchiardi, G. Spoto, P. D. C. Dietzel, S. Bordiga and A. Zecchina, *J. Am. Chem. Soc.*, 2008, **130**, 8386-8396.
4. M. Dincă, A. Dailly, Y. Liu, C. M. Brown, D. A. Neumann and J. R. Long, *J. Am. Chem. Soc.*, 2006, **128**, 16876-16883.
5. T. K. A. Hoang, L. Morris, J. Sun, M. L. Trudeau and D. M. Antonelli, *Journal of Materials Chemistry A*, 2013, **1**, 1947-1951.
6. T. K. A. Hoang, L. Morris, J. M. Rawson, M. L. Trudeau and D. M. Antonelli, *Chem. Mater.*, 2012, **24**, 1629-1638.
7. A. Hamaed, T. K. A. Hoang, G. Moula, R. Aroca, M. L. Trudeau and D. M. Antonelli, *J. Am. Chem. Soc.*, 2011, **133**, 15434-15443.
8. T. K. A. Hoang, A. Hamaed, G. Moula, R. Aroca, M. Trudeau and D. M. Antonelli, *J. Am. Chem. Soc.*, 2011, **133**, 4955-4964.
9. A. Hamaed, M. Trudeau and D. M. Antonelli, *J. Am. Chem. Soc.*, 2008, **130**, 6992-6999.
10. X. Hu, B. O. Skadtchenko, M. Trudeau and D. M. Antonelli, *J. Am. Chem. Soc.*, 2006, **128**, 11740-11741.
11. K. Pareek, Q. Zhang, R. Rohan, Z. Yunfeng and H. Cheng, *RSC Advances*, 2014, **4**, 33905-33910.
12. K. Pareek, Q. Zhang, R. Rohan, G. Xu and H. Cheng, *Advanced Materials Interfaces*, 2014 DOI 10.1002/admi.201400107.
13. B. Zheng, J. Bai, J. Duan, L. Wojtas and M. J. Zaworotko, *J. Am. Chem. Soc.*, 2010, **133**, 748-751.
14. Y. Yan, I. Telepeni, S. Yang, X. Lin, W. Kockelmann, A. Dailly, A. J. Blake, W. Lewis, G. S. Walker, D. R. Allan, S. A. Barnett, N. R. Champness and M. Schröder, *J. Am. Chem. Soc.*, 2010, **132**, 4092-4094.
15. C.-D. Wu, A. Hu, L. Zhang and W. Lin, *J. Am. Chem. Soc.*, 2005, **127**, 8940-8941.
16. B. Gómez-Lor, E. Gutiérrez-Puebla, M. Iglesias, M. A. Monge, C. Ruiz-Valero and N. Snejko, *Chem. Mater.*, 2005, **17**, 2568-2573.
17. T. Sawaki and Y. Aoyama, *J. Am. Chem. Soc.*, 1999, **121**, 4793-4798.
18. S.-H. Cho, B. Ma, S. T. Nguyen, J. T. Hupp and T. E. Albrecht-Schmitt, *Chem. Commun.*, 2006, 2563-2565.
19. M. Albrecht, M. Lutz, A. L. Spek and G. van Koten, *Nature*, 2000, **406**, 970-974.
20. J. A. Real, E. Andrés, M. C. Muñoz, M. Julve, T. Granier, A. Bousseksou and F. Varret, *Science*, 1995, **268**, 265-267.
21. L. G. Beauvais, M. P. Shores and J. R. Long, *J. Am. Chem. Soc.*, 2000, **122**, 2763-2772.
22. Y. H. Hu and L. Zhang, *Adv. Mater.*, 2010, **22**, E117-E130.
23. J. L. C. Rowsell and O. M. Yaghi, *Angew. Chem. Int. Ed.*, 2005, **44**, 4670-4679.
24. R. C. Lochan and M. Head-Gordon, *PCCP*, 2006, **8**, 1357-1370.
25. C. V. J. Skipper, D. M. Antonelli and N. Kaltsoyannis, *The Journal of Physical Chemistry C*, 2012.
26. M. P. Suh, H. J. Park, T. K. Prasad and D.-W. Lim, *Chem. Rev.*, 2011, **112**, 782-835.
27. H. Cheng, X. Sha, L. Chen, A. C. Cooper, M.-L. Foo, G. C. Lau, W. H. Bailey Iii and G. P. Pez, *J. Am. Chem. Soc.*, 2009, **131**, 17732-17733.
28. S. K. Bhatia and A. L. Myers, *Langmuir*, 2006, **22**, 1688-1700.
29. S. S. Kaye and J. R. Long, *J. Am. Chem. Soc.*, 2007, **130**, 806-807.
30. S. M. Cohen, *Chem. Rev.*, 2011, **112**, 970-1000.
31. D. Yuan, W. Lu, D. Zhao and H.-C. Zhou, *Adv. Mater.*, 2011, **23**, 3723-3725.
32. Z. Xiang and D. Cao, *Journal of Materials Chemistry A*, 2013, **1**, 2691-2718.
33. S. S. Han, H. Furukawa, O. M. Yaghi and W. A. Goddard, *J. Am. Chem. Soc.*, 2008, **130**, 11580-11581.
34. J. Lan, D. Cao, W. Wang, T. Ben and G. Zhu, *The Journal of Physical Chemistry Letters*, 2010, **1**, 978-981.
35. G. Yang, H. Han, C. Du, Z. Luo and Y. Wang, *Polymer*, 2010, **51**, 6193-6202.
36. M. G. Schwab, B. Fassbender, H. W. Spiess, A. Thomas, X. Feng and K. Müllen, *J. Am. Chem. Soc.*, 2009, **131**, 7216-7217.
37. K. Pareek, Q. Zhang, R. Rohan and H. Cheng, *Journal of Materials Chemistry A*, 2014, **2**, 13534-13540.
38. K. Sumida, C. M. Brown, Z. R. Herm, S. Chavan, S. Bordiga and J. R. Long, *Chem. Commun.*, 2011, **47**, 1157-1159.
39. P. Parilla, *http://www.hydrogen.energy.gov/pdfs/review12/st014_parilla_2012_o.pdf*, **Hydrogen Sorbent Measurement Qualification and Characterization**
40. D. P. M. Broom, P., *J. Alloys Compd.*, 2007, **446–447**, 687-691.
41. A. P. Katsoulidis and M. G. Kanatzidis, *Chem. Mater.*, 2011, **23**, 1818-1824.
42. *NIST X-ray Photoelectron Spectroscopy Database, Version 4.1 (National Institute of Standards and Technology, Gaithersburg, 2012);*.
43. A. Deryło-Marczewska, J. Goworek, S. Pikus, E. Kobylas and W. Zgrajka, *Langmuir*, 2002, **18**, 7538-7543.
44. G. Coullerez, D. Léonard, S. Lundmark and H. J. Mathieu, *Surf. Interface Anal.*, 2000, **29**, 431-443.
45. P. Pandey, A. P. Katsoulidis, I. Eryazici, Y. Wu, M. G. Kanatzidis and S. T. Nguyen, *Chem. Mater.*, 2010, **22**, 4974-4979.
46. M. G. Schwab, D. Crespy, X. Feng, K. Landfester and K. Müllen, *Macromol. Rapid Commun.*, 2011, **32**, 1798-1803.
47. R. Ströbel, J. Garche, P. T. Moseley, L. Jörissen and G. Wolf, *J. Power Sources*, 2006, **159**, 781-801.
48. J. R. Holst, A. Trewin and A. I. Cooper, *Nat Chem*, 2010, **2**, 915-920.

49. Y. Peng, G. Srinivas, C. E. Wilmer, I. Eryazici, R. Q. Snurr, J. T. Hupp, T. Yildirim and O. K. Farha, *Chem. Commun.*, 2013, **49**, 2992-2994.